

# Fly Ash Capture of Mercuric Chloride Vapors from Exhaust Combustion Gas

DESPINA KARATZA,<sup>†</sup>  
AMEDEO LANCIA,<sup>\*,†</sup> AND  
DINO MUSMARRA<sup>‡</sup>

*Dipartimento di Ingegneria Chimica, Università di Napoli "Federico II", P.le Tecchio 80, 80125 Napoli, Italy, and  
Istituto di Ricerche sulla Combustione, CNR, P.le Tecchio 80, 80125 Napoli, Italy*

Emissions of mercuric chloride from incineration of Municipal Solid Waste (MSW) constitute a severe environmental problem. Recent studies of the emissions from MSW incinerators indicate that, when fabric filters are used, fly ash may promote Hg emission control. In this investigation, a laboratory-scale apparatus was used to evaluate HgCl<sub>2</sub> adsorption on MSW fly ash. A mixture of N<sub>2</sub> and HgCl<sub>2</sub> was used as gas phase, with HgCl<sub>2</sub> concentration varying between 0.5 and 10 mg/m<sup>3</sup>. Fly ash samples collected, on the fabric filter of an industrial size MSW incinerator, were tested to understand the mechanisms involved in mercury fly ash sorption. The experiments led to the determination of the breakthrough curves for the fixed bed and of the adsorption isotherms at different temperatures in the range of 150–250 °C. The adsorption isotherms, which have a characteristic "Langmuir" shape, were used to evaluate the Langmuir parameters at the temperatures investigated and the heat of adsorption for the phenomenon.

## Introduction

Mercury is a pollutant particularly dangerous for human health because it is a mutagenic and teratogenic agent and furthermore is a strong neurological and behavioral toxicant (1). Mercury compounds are emitted into the atmosphere from various anthropogenic and natural sources and are removed through dry and wet deposition processes. Mercury deposited on soil and in water bodies may bioconcentrate in vegetation and fish (1, 2); consumption of produce and fish may lead to adverse health effects on humans and on predator animals (3).

The main sources of anthropogenic mercury emissions to the atmosphere are exhaust gases from coal combustion and municipal solid waste (MSW) incineration. Mercury is a trace element both in coal (0.1–0.3 mg Hg/kg) and in MSW (0.5–3 mg Hg/kg) (4). During combustion, most of mercury (up to 98%) is volatilized and is emitted in the gaseous phase either in the metallic or in the oxidized form (5). Experimental measurements (6, 7) and thermodynamic analysis (8) indicate that in flue gas from MSW incinerators mercury is mainly found as HgCl<sub>2</sub>, probably due to the relatively high concentration of HCl in the gas. On the contrary, elemental mercury

is the prevailing form in emissions from coal combustion processes as consequence of the relatively high concentration of SO<sub>2</sub> (6, 9).

Mercury adsorption from flue gas is the most common approach to meet air quality standards, due to the low cost inertization and discharge of the solid waste. With the aim of increasing the efficiency of the dry mercury removal processes, the attention of many researchers was focused on the interactions between mercury vapors and adsorbing materials both from a kinetic and a thermodynamic point of view. Adsorption of oxidized mercury was studied by Schager (7), who found that oxidized mercury is more easily adsorbed than elemental mercury. Lancia et al. (8), adsorbing mercuric chloride on calcium hydroxide, found that the lower the temperature, the higher the adsorption capacity. Karatza et al. (10–12), studying the adsorption of HgCl<sub>2</sub> on activated carbon and on the same carbon impregnated with Na<sub>2</sub>S, found that impregnation of carbon strongly enhances the adsorption capacity and that the adsorption process is exothermic for both sorbent. Karatza et al. (13) used as sorbent *Sorbalit*, a mixture of impregnated activated carbon and Ca(OH)<sub>2</sub>, expressly designed to capture both mercury vapors and acid gases. They showed that the adsorption capacity depends on temperature in an unusual fashion: it decreases for 70° < T < 150 °C and then increases for 150° < T < 250 °C. Physical adsorption occurs for T < 150 °C, while for T > 150 °C the results fall in a "transition zone" between physical adsorption and chemical adsorption. Tseng et al. (14) studied the mercury removal in a full-scale incineration plants. They found highly variable Hg collection efficiencies (ranging from 0 to 95%) and indicated that the key parameter affecting Hg removal is the presence, downstream of the acid gas control unit, of a fabric filter for particulate collection. This result was interpreted by making the hypothesis that the solid particulate collected (a mixture of fly ash and calcium compounds) can adsorb HgCl<sub>2</sub> and that fabric filters allow enough contact time between the gas phase and the solid cake deposited on the filter tissue. Furthermore, they also report that the operating temperature of the filter has to be kept as low as possible, being the adsorption phenomenon strongly sensitive to temperature. However it appears that there is a lack of quantitative information about HgCl<sub>2</sub> capture by fly ash and about the mechanisms through which such capture occurs.

The main objective of the present work has been the study of the adsorption capacity shown by fly ash collected on the fabric filter operating in a full scale MSW incinerator located in Northern Italy. Different ash samples were compared each other with regard the HgCl<sub>2</sub> adsorption capacity. The adsorption isotherms and the breakthrough curves for the materials tested were determined varying the temperature in the range of 150–250 °C and the HgCl<sub>2</sub> concentration in the range of 0.5–10 mg/m<sup>3</sup>. Eventually, the Langmuir parameters for the adsorption isotherms were determined, and a model based on the assumption of kinetic control was used to evaluate the kinetic parameters of the process.

## Experimental Section

Experiments were performed using the laboratory scale apparatus shown in Figure 1. In this apparatus the gas stream at the required temperature and HgCl<sub>2</sub> concentration was produced, and the HgCl<sub>2</sub> capture on a fixed bed of adsorbent material was performed. The gas stream was obtained by sublimating reagent grade solid HgCl<sub>2</sub> contained in a stainless steel (AISI 316) cylindrical saturator into a stream of pure nitrogen. The saturator was kept at a fixed temperature by

\* Corresponding author phone: [39](81)768-2243; fax: [39](81)-593-6936; e-mail: lancia@unina.it.

<sup>†</sup> Università di Napoli "Federico II".

<sup>‡</sup> Istituto di Ricerche sulla Combustione.

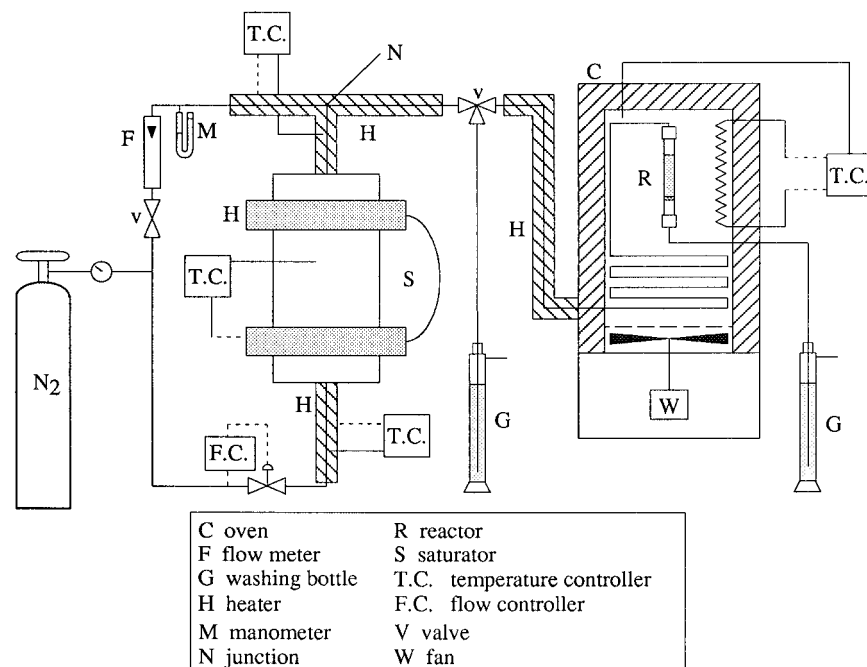


FIGURE 1. Sketch of the experimental apparatus.

a heating tape driven by a PID temperature controller, and the mass flow rate of the  $\text{N}_2$  stream was kept constant by a hot wire flow rate controller. The  $\text{HgCl}_2$  concentration in the gas stream fed to the reactor was controlled by varying the temperature of the saturator and by diluting the saturated stream with a stream of pure nitrogen in the junction N. The diluted stream was fed to a cylindrical glass reactor (35 mm ID) kept into a thermostated oven equipped with a PID temperature controller. To avoid  $\text{HgCl}_2$  reduction (15) steel surfaces in contact with a gas phase containing mercuric chloride are kept at a temperature lower than  $50^\circ\text{C}$ ; downstream the junction N, where the temperature is higher than  $50^\circ\text{C}$ , surfaces (ducts and reactor) are made of Pyrex glass.

The reactor contained the adsorbing bed, made of about 50 mg of fly ash mixed with 3.0 g of inert glass beads with similar size. The thickness of the bed ( $L$ ) was 2.5 mm, and additional 57.5 mm of glass beads were provided upstream to the bed in order to distribute the gas flow over the entire cross section. A downward flow was chosen for the gas in order to avoid losses of powder in the gas stream.

The experiments were conducted varying the  $\text{HgCl}_2$  concentration in the inlet stream to the bed ( $c_0$ ) in the range of  $0.5\text{--}10.0\text{ mg/m}^3$  and varying the bed temperature from  $150\text{--}250^\circ\text{C}$ , while keeping the gas flow rate fixed at  $8.33 \times 10^{-5}\text{ m}^3/\text{s}$ . Blank tests, performed at each temperature and  $\text{HgCl}_2$  gas concentration, showed that reactor and glass beads could adsorb less than 1% of mercury fed. Before each run, the gas line was saturated for about 2 h with a gas having the same concentration and temperature as those to be used in the experiment. This procedure was adopted since the steel ducts upstream the junction N can adsorb  $\text{HgCl}_2$  vapors (7). The  $\text{HgCl}_2$  concentration in outlet gas stream ( $c_{\text{out}}$ ) was determined by absorbing the gas by means of gas washing bottles for about 1 min. An aqueous solution containing  $\text{KMnO}_4$  acidified by  $\text{H}_2\text{SO}_4$  was used (16), and the samples were analyzed by means of Cold Vapor Atomic Absorption (CVAA), using  $\text{NaBH}_4$  as reducing agent. Such a procedure was considered accurate, since no mercury was found in the gas exiting the washing bottle when another bottle was placed in series to the first.

At the beginning of each experimental run (i.e. after saturation of the gas line),  $c_0$  was determined. Afterward  $c_{\text{out}}$

was measured at different times, until saturation was reached ( $c_{\text{out}} = c_0$ ). The longest saturation time found was of about 1 h; therefore, to be sure that the saturation of the solid had been reached, it was decided to continue each experiment for a time much longer than the saturation time, namely 5 h.

After each run the total adsorbate loading at saturation ( $\omega^*$ ) was measured by leaching the bed material with *aqua regia* ( $\text{HNO}_3 + 3\text{HCl}$ ) and then by analyzing the solution by means of CVAA, and an error not larger than 8% was found in the mercury material balance.

## Results

Fly ash collected on the fabric filter of a full scale MSW incinerator located in Northern Italy was used as sorbent. The incinerator has an average potentiality of 120 ton/day and is equipped with a lime spray-dryer to control acid gas emissions, followed by a fabric filter for particulate removal. A first objective of this work was to have reliable information about the characteristics of the fly ash produced by the plant, with the aim of linking such characteristics to the  $\text{HgCl}_2$  adsorbing capacity. Seven different samples, individuated by the letters from "A"–"G", were taken in different days of operation of the incinerator and used for the present study. The reason for using different fly ash samples depends on the fact that both the composition of the waste fed to the incinerator and the operating conditions of the incineration process vary from day to day, and this is reflected in the characteristics of the ash produced. Fly ash physical properties and chemical composition have been measured. The elemental composition of the fly ash varies from day to day; therefore the chemical speciation of the various samples are reported in Table 1. On the contrary, physical properties are quite constant hence the average values are given: the bulk density ( $\rho_b$ ) is  $817\text{ kg/m}^3$ , the volume averaged diameter ( $d_{50}$ ) is  $38\text{ }\mu\text{m}$ , and the BET specific surface area ( $a_s$ ) is  $49\text{ m}^2/\text{g}$ .

Preliminary adsorption runs were performed at  $150^\circ\text{C}$  to compare the  $\text{HgCl}_2$  adsorption capacity of the seven fly ash samples. The results of such runs are presented in Table 2, which reports the  $\text{HgCl}_2$  inlet concentration, the adsorbate loading at saturation, and the ratio  $\omega^*/c_0$ . It has been

TABLE 1. Chemical Composition of the Fly Ash Samples Considered (%<sub>w/w</sub>)

ash sample	SiO <sub>2</sub>	CaO	MgO	Al <sub>2</sub> O <sub>3</sub>	SO <sub>3</sub>	C	H	Fe	Pb	Zn	Cd	Ni	Mn	Cu
"A"	19.1	36.6	2.37	11.64	10.56	0.61	0.23	1.53	0.85	1.47	0.029	0.032	0.070	0.130
"B"	20.1	36.5	2.57	16.31	9.20	0.57	0.30	1.41	0.86	1.51	0.038	0.020	0.040	0.140
"C"	18.2	31.6	2.35	18.53	8.48	1.08	0.28	1.45	1.00	1.38	0.056	0.018	0.075	0.013
"D"	18.8	36.6	0.33	17.92	10.03	0.71	0.30	1.40	0.77	1.48	0.022	0.020	0.063	0.095
"E"	18.6	32.0	1.70	9.15	9.15	0.55	0.30	1.44	0.81	1.33	0.046	0.041	0.076	0.130
"F"	20.7	32.6	1.60	7.60	7.60	0.68	0.28	1.46	0.65	1.09	0.042	0.025	0.082	0.110
"G"	18.2	35.1	0.69	9.90	9.91	0.73	0.32	1.47	0.82	1.08	0.045	0.024	0.073	0.120

TABLE 2. Adsorption Capacities at 150 °C for the Fly Ash Samples under Investigation

fly ash sample	$c_0$ (mg/m <sup>3</sup> )	$\omega^* \times 10^3$ (g/g)	$\omega^*/c_0$ (m <sup>3</sup> /g)
"A"	1.65	0.59	0.36
"B"	1.44	1.18	0.82
"C"	1.40	1.14	0.81
"D"	1.38	1.16	0.84
"E"	1.63	0.64	0.39
"F"	1.34	0.42	0.31
"G"	1.40	0.53	0.38

necessary to include such a ratio in the table since, due to the characteristics of the experimental apparatus used, the inlet HgCl<sub>2</sub> concentration to the reactor was not constant in all the experiments, and therefore a direct comparison among  $\omega^*$ 's is not possible.

Data in Table 2 show that the adsorption capacities of the fly ash samples considered vary within quite a wide range and in particular that the ratio  $\omega^*/c_0$  for samples "B", "C", and "D" is more than doubled with respect to the corresponding value for samples "A", "E", "F", and "G". On the basis of the experimental results, it is quite complex to explain such a difference in the adsorption capacity and at the moment not completely exhaustive. Indeed, changing the ash sample the surface area does not vary significantly, and neither the carbon or the calcium oxide, which are considered in the literature as effective sorbent for mercury (8, 12), seems able to justify the doubling in the adsorption capacity. The Al<sub>2</sub>O<sub>3</sub> content is bigger for the ash samples "B"–"D"; therefore, it seems possible that such a variable plays a relevant role in determining the adsorption capacity of the fly ash, even though further studies are necessary to confirm such conclusion.

Using a "worst case" approach to the problem of HgCl<sub>2</sub> adsorption on fly ash, sample "A", i.e. one of the samples with low adsorbing capacity, was selected for a more extensive study. In particular it was used for a series of experimental runs in which HgCl<sub>2</sub> adsorption was studied varying both bed temperature and inlet concentration to the bed. The breakthrough curves were obtained by measuring the HgCl<sub>2</sub> concentration in the outlet stream from the reactor at different times, and it was assumed that thermodynamic equilibrium had been reached when the outlet concentration became equal to the inlet concentration. Breakthrough curves for the bed temperatures of 150, 200, and 250 °C are reported in Figures 2–4 as ratio of the outlet to the inlet concentration ( $c_{out}/c_0$ ) versus time. Altogether, the results reported in Figures 2–4 show that the time necessary for saturation, which is a function of the bed temperature and of gas flow rate and concentration, is in the order of 1 h, and that increasing the HgCl<sub>2</sub> concentration in the gas phase the time necessary to reach the saturation becomes shorter. Furthermore, the comparison among Figures 2–4 evidences that the higher the temperature the lower the saturation time.

Data in Figures 2–4 allow the evaluation of the amount of mercury found on the solid at saturation, which represents

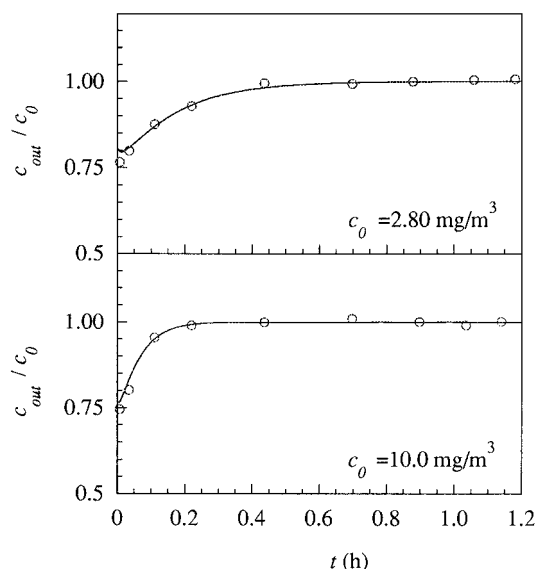


FIGURE 2. Breakthrough curves for fly ash sample "A" with a bed temperature of 150 °C: ○, experimental measurements; —, model results.

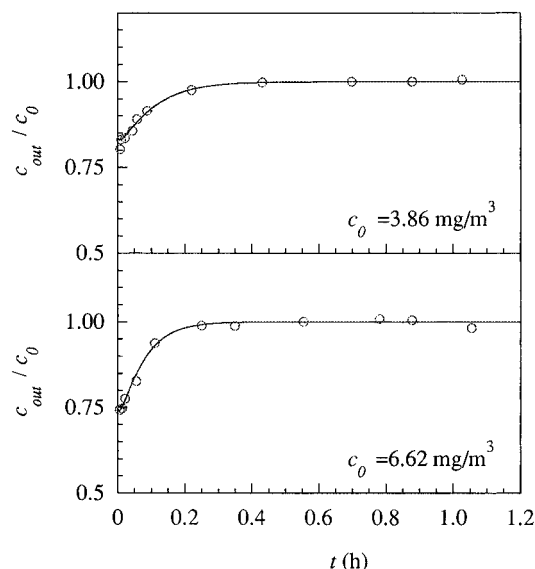


FIGURE 3. Breakthrough curves for fly ash sample "A" with a bed temperature of 200 °C: ○, experimental measurements; —, model results.

the adsorbate loading in thermodynamic equilibrium with the gas phase at concentration  $c^*$ . Values of  $\omega^*$  obtained for different concentrations of the gas stream give the adsorption isotherms reported in Figure 5 for the three temperatures of 150, 200, and 250 °C. The isotherms show that the higher the temperature the lower the adsorption capacity, in agreement with the exothermic nature typical of adsorption processes.

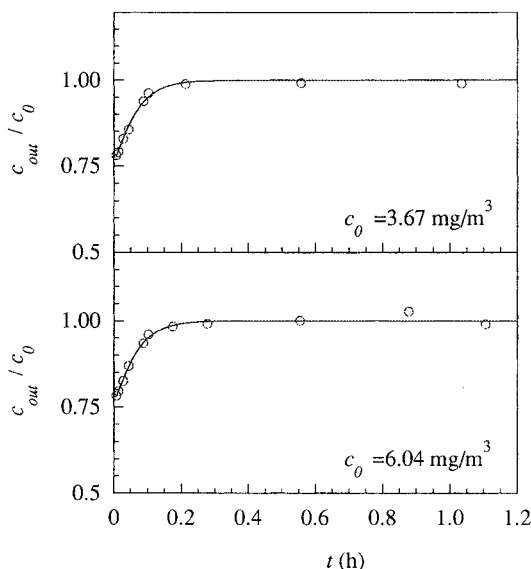


FIGURE 4. Breakthrough curves for fly ash sample "A" with a bed temperature of 250 °C: ○, experimental measurements; —, model results.

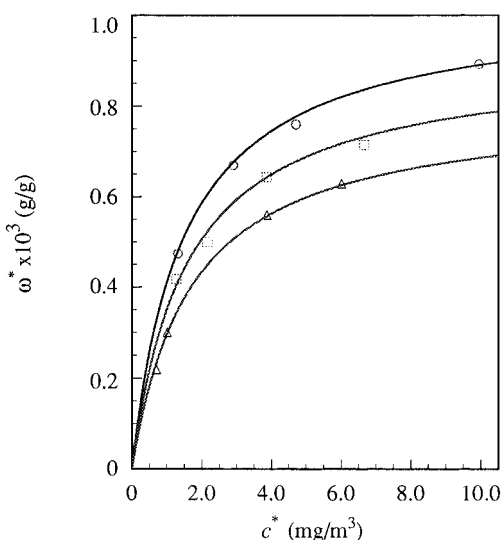
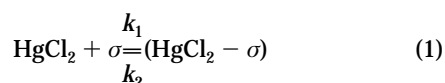


FIGURE 5. Adsorption isotherms for fly ash sample "A" at different temperatures: ○,  $T = 150$  °C; □,  $T = 200$  °C; △,  $T = 250$  °C; —, Langmuir isotherms ( $R^2_{150^\circ\text{C}} = 0.98$ ;  $R^2_{200^\circ\text{C}} = 0.99$ ;  $R^2_{250^\circ\text{C}} = 0.98$ ).

## Discussion

The experimental results show that  $\omega^*$  depends on  $c^*$  and therefore that the phenomenon under consideration is an adsorption process rather than a gas–solid reaction. The adsorption process can be described using the pseudoreaction between gaseous  $\text{HgCl}_2$  and active sites " $\sigma$ " placed on the surface of the materials constituting the fly ash samples:



Using the Langmuir isotherm to describe the fly ash– $\text{HgCl}_2$  interaction, the rate of the process can be expressed as the difference between the adsorption rate and the desorption rate. The former is proportional to  $\text{HgCl}_2$  concentration in the gas phase and to the difference between the number of sites available for adsorption and the number of occupied sites, while the latter is simply proportional to the number of occupied active sites; hence the overall rate

TABLE 3. Thermodynamic and Kinetic Constants for  $\text{HgCl}_2$  Adsorption on Fly Ash Sample "A" at Different Temperatures

$T$ (°C)	$K$ (m <sup>3</sup> /g)	$\omega_{\max} \times 10^3$ (g/g)	$k_1$ (m <sup>3</sup> /g s)	$k_2$ (s <sup>−1</sup> )
150	672	1.03	0.37	$5.5 \times 10^{-4}$
200	632	0.91	0.46	$7.3 \times 10^{-4}$
250	586	0.80	0.57	$9.7 \times 10^{-4}$

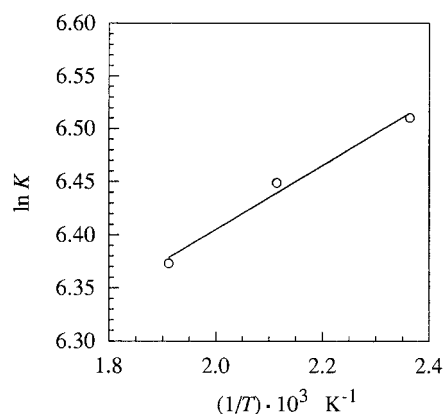


FIGURE 6. Thermodynamic equilibrium constant for fly ash sample "A" versus the inverse of absolute temperature: ○ data of Table 4; —eq 5 ( $R^2 = 0.98$ ).

is expressed by the following equation

$$r = k_1(\omega_{\max} - \omega)c - k_2\omega \quad (2)$$

where  $c$  is the  $\text{HgCl}_2$  concentration in the gas phase,  $\omega$  is its concentration as adsorbate on the solid,  $\omega_{\max}$  is the asymptotic adsorbate concentration, and  $k_1$  and  $k_2$  are the kinetic constants of the adsorption and of the desorption reaction, respectively. At equilibrium ( $r = 0$ ) such rate equation leads to the well-known Langmuir isotherm

$$\omega^* = \omega_{\max} \frac{Kc^*}{1 + Kc^*} \quad (3)$$

where  $K$  is the equilibrium constant, related to the kinetic parameters by the equation

$$K = k_1/k_2 \quad (4)$$

The equilibrium data of Figure 5 were used to evaluate the Langmuir parameters for the different temperatures under investigation. Using a nonlinear regression such parameters were calculated and are reported in Table 3. The Langmuir isotherms are also included in Figure 5 (continuous lines). The values reported in Table 3 show that both  $K$  and  $\omega_{\max}$  decrease when temperature increases. In particular, in agreement with the physical meaning of the equilibrium constant  $K$ , it is possible to hypothesize a dependence on the temperature of the Arrhenius type, according to the following equation (17)

$$K = K_0 \exp\left(-\frac{\Delta H_{\text{ads}}}{RT}\right) \quad (5)$$

where  $K_0$  is the preexponential factor and  $\Delta H_{\text{ads}}$  is the heat of adsorption. A nonlinear regression gave for  $K_0$  the value of 330 m<sup>3</sup>/g, and for  $\Delta H_{\text{ads}}$  the value of −2.5 kJ/mol. The values of  $K$  are reported in Figure 6 in the form of an "Arrhenius" plot together with the continuous line obtained using eq 5.

The values of the kinetic constants  $k_1$  and  $k_2$  can be evaluated from the experimental breakthrough data, con-



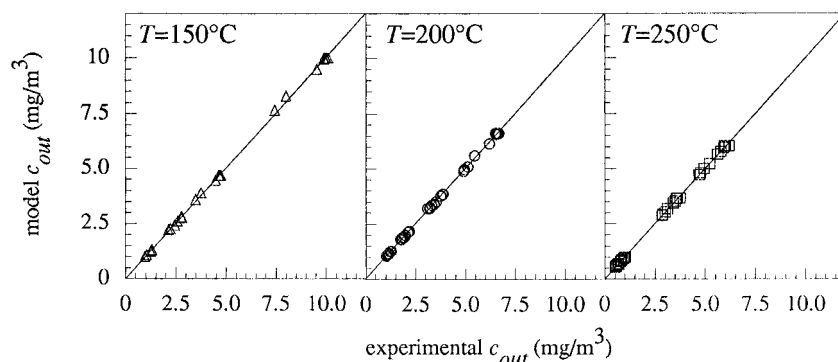


FIGURE 7. Comparison between model and experimental  $\text{HgCl}_2$  outlet concentration:  $\triangle$ ,  $T = 150^\circ\text{C}$ ;  $\circ$ ,  $T = 200^\circ\text{C}$ ;  $\diamond$ ,  $T = 250^\circ\text{C}$ .

sidering a balance on  $\text{HgCl}_2$  adsorbed in the bed. Indicating the axial coordinate in the bed with  $x$  and the time with  $t$ , it is

$$V \frac{\partial c}{\partial x} + \epsilon \frac{\partial c}{\partial t} + \rho_b \frac{\partial \omega}{\partial t} = 0 \quad (6)$$

where  $V$  is the gas superficial velocity, which is assumed constant along the reactor, and  $\epsilon$  is the external void fraction of the bed. Such balance equation has to be associated to a constitutive equation for the rate of accumulation on the solid: neglecting the diffusional resistances and considering eq 2, the constitutive equation can be expressed as follows:

$$\frac{\partial \omega}{\partial t} = k_1(\omega_{\max} - \omega)c - k_2\omega \quad (7)$$

Equations 6 and 7 have to be integrated subject to the following boundary conditions:

$$\begin{cases} t = 0; & 0 \leq x \leq L; & c = 0; & \omega = 0 \\ t \geq 0; & x = 0; & c = c_0 \end{cases} \quad (8)$$

The system of eqs 6–8 was solved using the analytical method proposed by Rhee et al. (18). Using the values of  $K$  and  $\omega_{\max}$  experimentally determined for the different temperatures, the  $\text{HgCl}_2$  concentration profiles both in the gas and on the solid phase could be obtained as a function of time. A comparison between model and experimental results was possible in terms of  $c_{\text{out}}$  and  $\omega_{\text{tot}}$ . The only parameter in such equations is  $k_1$ , which was estimated by fitting model calculations to experimental breakthrough curves. Values of  $k_1$ , together with values of  $k_2$  obtained by eq 4, are also reported in Table 3. Furthermore, breakthrough curves calculated by eqs 6–8 are reported in Figures 2–4 (continuous lines). As expected the values of  $k_1$  and  $k_2$  significantly depend on bed temperature but are independent of the  $\text{HgCl}_2$  inlet concentration to the adsorbing bed. Such observation is in good agreement with the physical meaning of these parameters, the value of which is not expected to be affected by the  $\text{HgCl}_2$  concentration in the gas phase. This result is well shown in Figure 7, which reports, for the three temperature of interest in this work, a comparison between the experimental values of  $c_{\text{out}}$  and the calculated ones, evidencing a good agreement between model and experiments.

The comparison between the experimental results presented in Figure 5 and those reported in the other papers devoted to  $\text{HgCl}_2$  adsorption (7, 8, 13, 14) is difficult since those papers do not report equilibrium data readily comparable with the adsorption isotherms of Figure 5. The comparison between fly ash equilibrium data and that obtained by Karatz et al. (12), using “raw” activated carbon and the same carbon impregnated with  $\text{Na}_2\text{S}$ , is possible in terms of  $K$  and  $\omega_{\max}$ . In particular, for all sorbent materials, the  $\text{HgCl}_2$  adsorption is an exothermic process, and  $K$  values

are of the same order of magnitude. On the contrary, comparing  $\omega_{\max}$  values it appears that the fly ash  $\omega_{\max}$  is 10 times lower than that for the carbon; this would suggest that fly ash may be considered a sorbent less effective than activated carbon. However, considering that fly ash is already available in the incineration plants at no cost and in any case they have to be inertized before discarding, the amount of mercury adsorbed on fly ash reduce the cost of the mercury removal treatment.

### Acknowledgments

The authors wish to express their gratitude to Prof. Cesare Musmarra, who performed the chemical analysis of the ash.

### Nomenclature

$a_s$	surface area ( $\text{m}^2/\text{g}$ )
$c$	$\text{HgCl}_2$ concentration ( $\text{g}/\text{m}^3$ )
$d_{50}$	volume average diameter (m)
$k_1$	kinetic constant of the adsorption reaction ( $\text{m}^3/\text{g s}$ )
$k_2$	kinetic constant of the desorption reaction ( $\text{s}^{-1}$ )
$K$	equilibrium constant ( $\text{m}^3/\text{g}$ )
$K_0$	preexponential factor ( $\text{m}^3/\text{g}$ )
$L$	length of the adsorbing bed (m)
$R$	gas constant ( $\text{J}/\text{mol K}$ )
$R^2$	correlation coefficient (—)
$r$	adsorption rate ( $\text{s}^{-1}$ )
$t$	time (s)
$T$	temperature ( $^\circ\text{C}$ )
$V$	superficial velocity (m/s)
$x$	axial coordinate in the bed (m)

### Greek Symbols

$\Delta H_{\text{ads}}$	heat of adsorption ( $\text{kJ}/\text{mol}$ )
$\epsilon$	external void fraction (—)
$\rho_b$	bulk density ( $\text{g}/\text{m}^3$ )
$\omega$	adsorbate loading ( $\text{g}_{\text{HgCl}_2}/\text{g}_{\text{sorbent}}$ )
$\omega_{\max}$	asymptotic adsorbate concentration ( $\text{g}_{\text{HgCl}_2}/\text{g}_{\text{sorbent}}$ )

### Superscripts

*	equilibrium
---	-------------

### Subscripts

0	inlet
out	outlet
tot	total

## Literature Cited

- (1) Carpi, A.; Weinstein, L. H.; Ditz, D. W. *J. Air Waste Manage. Assoc.* **1994**, *44*, 669–672.
- (2) Roberts, R. H. *Food Safety*; Wiley and Sons: New York, 1981.
- (3) Seigneur, C.; Wrobel, J.; Costantinou, E. *Environ. Sci. Technol.* **1994**, *28*, 1589–1597.
- (4) Lindqvist, O. *Waste Manage. Res.* **1986**, *4*, 35–39.
- (5) Meij, R. *Water Air Soil Pollut.* **1991**, *56*, 21–33.
- (6) Hall, B.; Lindqvist, O.; Ljungstrom, E. *Environ. Sci. Technol.* **1990**, *24*, 108–111.
- (7) Schager, P. Ph.D. Dissertation, University of Goteborg: Goteborg, Sweden, 1990.
- (8) Lancia, A.; Musmarra, D.; Pepe, F.; Volpicelli, G. *Combust. Sci. Technol.* **1993**, *93*, 277–289.
- (9) Pacyna, J. M.; Munch J. *Water Air Soil Pollut.* **1991**, *56*, 51–61.
- (10) Karatza, D.; Lancia, A.; Musmarra, D.; Pepe, F. In *Twenty-Sixth Symposium (International) on Combustion*; The Combustion Institute: Pittsburgh, PA, U.S.A., 1996; pp 2439–2445.
- (11) Karatza, D.; Lancia, A.; Musmarra, D.; Pepe, F.; Volpicelli, G. *Combust. Sci. Technol.* **1996**, *112*, 163–174.
- (12) Karatza, D.; Lancia, A.; Musmarra, D.; Pepe, F.; Volpicelli, G. *Hazard. Waste Hazard. Mater.* **1996**, *13*, 95–105.
- (13) Karatza, D.; Lancia, A.; Musmarra, D.; Pepe, F. *J. Chem. Eng. Jpn.* **1996**, *29*, 939–946.
- (14) Tseng, C.; Chang, C.; Sedman, C. *AIChE Summer Meeting*; San Diego, CA, August 20, 1990.
- (15) Hall, B.; Lindqvist, O.; Ljungstrom, E. *Environ. Sci. Technol.* **1990**, *24*, 108–111.
- (16) Wilshire, N.; Knoll, J. E.; Ward, T. E. *J. Air Waste Manage. Assoc.* **1993**, *43*, 117–119.
- (17) Carrà, S.; Morbidelli, M. *Chimica Fisica Applicata*; Hoepli: Milan, Italy, 1983.
- (18) Rhee, H. K.; Aris, R.; Amundson, N. R. *First-Order Partial Differential Equations: Volume I*; Prentice Hall: Englewood Cliffs, NJ, U.S.A., 1986.

*Received for review December 11, 1997. Revised manuscript received August 17, 1998. Accepted September 2, 1998.*

ES971074M